Histochemistry and Cell Biology (2023) 160:321–339
https://doi.org/10.1007/s00418-023-02208-2

ORIGINAL PAPER

Effects of experimental ulcerative colitis on myenteric neurons in P2X7-knockout mice

Felipe Alexandre Machado[1] · Roberta Figueiroa Souza[1] · Vanessa Ribeiro Figliuolo[2] · Robson Coutinho-Silva[2] · Patricia Castelucci[1]

Accepted: 15 May 2023 / Published online: 12 June 2023

Abstract

This study aimed to investigate the distal colon myenteric plexus and enteric glial cells (EGCs) in P2X7 receptor-deficient (P2X7−/−) animals after the induction of experimental ulcerative colitis. 2,4,6-Trinitrobenzene sulfonic acid (TNBS) was injected into the distal colon of C57BL/6 (WT) and P2X7 receptor gene-deficient (P2X7−/−, KO) animals. Distal colon tissues in the WT and KO groups were analyzed 24 h and 4 days after administration. The tissues were analyzed by double immunofluorescence of the P2X7 receptor with neuronal nitric oxide synthase (nNOS)-immunoreactive (ir), choline acetyltransferase (ChAT)-ir, and PGP9.5 (pan neuronal)-ir, and their morphology was assessed by histology. The quantitative analysis revealed 13.9% and 7.1% decreases in the number of P2X7 receptor-immunoreactive (ir) per ganglion in the 24 h-WT/colitis and 4 day-WT/colitis groups, respectively. No reduction in the number of nNOS-ir, choline ChAT-ir, and PGP9.5-ir neurons per ganglion was observed in the 4 day-KO/colitis group. In addition, a reduction of 19.3% in the number of GFAP (glial fibrillary acidic protein)-expressing cells per ganglion was found in the 24 h-WT/colitis group, and a 19% increase in the number of these cells was detected in the 4 day-WT/colitis group. No profile area changes in neurons were observed in the 24 h-WT and 24 h-KO groups. The 4 day-WT/colitis and 4 day-KO/colitis groups showed increases in the profile neuronal areas of nNOS, ChAT, and PGP9.5. The histological analysis showed hyperemia, edema, or cellular infiltration in the 24 h-WT/colitis and 4 day-WT/colitis groups. Edema was observed in the 4 day-KO/colitis group, which showed no histological changes compared with the 24 h-KO/colitis group. We concluded that ulcerative colitis differentially affected the neuronal classes in the WT and KO animals, demonstrating the potential participation and neuroprotective effect of the P2X7 receptor in enteric neurons in inflammatory bowel disease.

Keywords P2X7 receptor · Myenteric neurons · Experimental ulcerative colitis · P2X7 knockout mouse

Introduction

The enteric nervous system (ENS) controls the functions of the gastrointestinal tract (GT) (for reviews, see Furness 2006, 2012). Enteric glial cells (EGCs) have been observed in myenteric and submucosal plexuses, in longitudinal, circular muscles and mucosa (Rühl 2005; Gulbransen and Sharkey 2012).

The markers of EGCs include S100B, a Ca^{2+} binding protein (Ferri et al. 1982), and glial fibrillary acidic protein (GFAP) (Jessen Mirsky 1980). Studies have shown that EGCs immunoreactive (ir) for GFAP and S100B undergo changes in humans and animals with ulcerative colitis (Bassotti et al. 2007; Von Boyen 2011; da Silva et al. 2015).

Inflammatory bowel diseases (IBDs), such as Crohn's disease (CD) and ulcerative colitis, can be triggered by several factors. The etiology of these disorders may be related to genetic susceptibility, the body's immune response, and phenotypic pressures associated with the intestinal flora (Aniwan et al. 2017). Most individuals with IBD are between 20 and 40 years of age, and 201 and 238 of every 100,000 people may have CD and colitis, respectively, which results in the estimation that approximately one million Americans suffer from intestinal disorders (Kappelman et al. 2007;

✉ Patricia Castelucci
pcastel@usp.br

[1] Department of Anatomy, Institute Biomedical and Sciences, University of São Paulo, Av. Prof. Dr. Lineu Prestes, 2415, São Paulo CEP 05508-900, Brazil

[2] Federal University of Rio de Janeiro, Rio de Janeiro, Brazil

Aniwan et al. 2017). The literature has shown the importance of the ENS in the functional activity of the GT in experimental models of ulcerative colitis. Changes in intestinal motility, decreased neuronal density associated with necrosis and apoptosis, and changes in neurotransmission have been widely described (Sanovic et al. 1999; Cook et al. 2000; Poli et al. 2001; Schneider et al. 2001; Linden et al. 2005; da Silva et al. 2015, 2017; Venkataramana et al. 2015).

ATP binds to P2X receptors, of which there are seven types, i.e., P2X1 to P2X7 (Abbracchio et al. 2009). The P2X7 receptor has been detected in the ENS and EGCs (Hu et al. 2001; Gulbransen et al. 2012; da Silva et al. 2015, 2017). Brilliant Blue G, an antagonist of the P2X7 receptor, has been used to restore myenteric neurons following ischemia/reperfusion (Palombit et al. 2019; Mendes et al. 2023) and the induction of experimental ulcerative colitis (Evangelinellis et al. 2022).

Purinergic receptors are expressed in the context of gastrointestinal disorders, particularly during neuronal death, and cause intestinal dysfunction (Yiangou et al. 2001; Antonioli et al. 2013, 2014; Evangelinellis et al. 2022; Santos et al. 2022). Gulbransen et al. (2012) showed that P2X7 receptors contribute to the death of enteric neurons and proved that intestinal inflammation can cause disturbances in motility.

This work aimed to analyze the levels of nNOS, choline acetyltransferase (ChAT), and PGP9.5, EGCs, and histological changes in neurons in the distal colon in P2X7 receptor gene-deficient mice following the induction of experimental ulcerative colitis.

Materials and methods

All protocols used in the study were approved by the Ethics Committee on Animal Use of the Biomedical Science Institute of the University of São Paulo (Protocol 83/2017). Young male mice (body weight 20–25 g) were maintained under standard conditions at 21 °C and a 12 h light–dark cycle. All of the animals were provided water ad libitum.

Induction of ulcerative colitis

A total of 72 animals were used. The protocols used for the establishment of the colitis induction and control groups were described previously (Wirtz et al. 2007; Figliuolo et al. 2017). The mice were weighed before, at various intervals up to 24 h and on the fourth day following 2,4,6-trinitrobenzene sulfonic acid (TNBS) injection. The following eight groups were used in the study: 24 h-WT/sham ($n = 8$), 24 h-WT/colitis ($n = 8$), 24 h-KO/sham ($n = 10$), 24 h-KO/colitis ($n = 10$), 4 day-WT/sham ($n = 8$), 4 day-WT/colitis ($n = 8$), 4 day-KO/sham ($n = 10$), and 4 day-KO/colitis ($n = 10$) groups.

Macroscopic and microscopic colitis scores were determined using an adapted scoring system (Table 1) (Fabia et al. 1993; Evangelinellis et al. 2022). The disease activity indices (DAIs) of all the groups were evaluated (Nooh and Nour-Eldien 2016; Evangelinellis et al. 2022).

Segments of the distal colon were dissected and placed in phosphate-buffered saline (PBS) containing nicardipine (10–6 M, Sigma, USA) to inhibit tissue contraction. The tissues were opened along the mesenteric border, cleaned with PBS, and then placed with the mucosal side down onto a sheet of balsa wood and fixed overnight at 4 °C with 4% paraformaldehyde in sodium phosphate buffer 0.2 M (pH 7.3). After 24 h, the tissue was cleared of fixative with three 10-min washes in 100% dimethylsulfoxide (DMSO), followed by three 10-min washes in PBS. All tissue was stored at 4 °C in PBS containing sodium azide (0.1%). For immunohistochemistry, the myenteric plexus of the distal colon was preincubated with 10% normal horse serum in PBS containing 1.5% Triton X-100 for 45 min at room temperature. The antibodies used in this study are listed in Table 2. Double labelling was achieved using combinations of the antisera indicated in Table 2. After incubation with primary antisera, tissues were washed three times for 10 min in PBS and incubated with various secondary antibodies (Table 2). The PBS washes were repeated, and the tissue was mounted in buffered glycerol with 0.5 M sodium carbonate (pH 8.6) (da Silva et al. 2015; Evangelinellis et al. 2022; Mendes et al. 2023).

To detect the P2X7 receptor, we used rabbit antiserum raised against amino acids 576–595 of the P2X7 receptor, with a single Cys extension at the N-terminus (AB5246 from Millipore, Temecula, CA, USA). To confirm the specificity of the antibodies used, the antisera were diluted to working concentrations, combined with a synthetic peptide (N-cys-576-595, lot 2361386) from the P2X7 receptor and equilibrated at 4 °C overnight. Primary antisera to which no peptides absorbed were used in parallel experiments as controls.

The tissue specimens were examined using a Nikon 80i fluorescent microscope at ×40 magnification with numerical aperture 0.75 and aberration correction in the visible range. Preparations were examined on a Nikon 80i fluorescent microscope equipped with the appropriate filters. Characteristics of Filter Cube for Alexa 488: filter diameter 25 mm, excitation filter 480/30, dichroic mirror 505, and barrier filter 535/40. Characteristics of Filter Cube for Alexa Fluor 594: filter diameter 25 mm, excitation filter 560/40, dichroic mirror 600, and barrier filter 635/60. Characteristics of Filter Cube for DAPI: filter diameter 25 mm, excitation filter 375/28, dichroic mirror 415, and barrier filter 460/50.

Table 1 Macroscopic colonic injury scale (Bell et al. 1995), microscopic colonic injury scale (Fabia et al. 1993; Erdogan et al. 2003), and disease activity index (DAI) scale based on percentage weight change, stool consistency, and occult and/or rectal bleeding

Score	Macroscopic colonic injury
0	Normal
1	Presence of hyperemia without ulcers
2	Ulcerations without hyperemia
3	Ulcerations at one site
4	Ulcerations at two or more sites
5	Sites of damage extending > 1 cm
6–10	Sites of damage extending > 2 cm; the score increases by 1 for each additional cm
	Microscopic colonic injury
Score	*Ulcerations*
0	No ulceration
1	Single ulceration not exceeding the lamina muscularis mucosa
2	Ulcerations not exceeding the mucosa
3	Ulcerations exceeding the submucosa
Score	*Edema (submucosal)*
0	No edema
1	Mild edema
2	Moderate edema
3	Severe edema
Score	*Inflammatory cell infiltration*
0	No infiltration
1	Mild infiltration
2	Moderate infiltration
3	Dense infiltration
Disease activity index (DAI)	Percentage weight change, stool consistency, and occult and/or rectal bleeding*
Score	*Weight change (%)*
0	1%
1	1–5%
2	5–10%
3	10–15%
4	> 15%
Score	*Stool consistency (%)*
0	Normal[a] (well-formed pellets)
1	Normal
2	Loose stool[b] (pasty and semiformed stools that did not stick to the anus)
3	Loose stool
4	Diarrhea[c] (liquid stools that stuck to the anus)
Score	*Occult/gross rectal bleeding*
0	Normal
1	Occult blood +
2	Occult blood ++
3	Occult blood +++
4	Gross bleeding

*The DAI was calculated by summing the scores for these parameters (da Silva et al. 2015; Nooh and Nour-Eldien 2016; Evangelinellis et al. 2022). [a] well-formed pellets; [b] pasty and semiformed stools that did not stick to the anus; [c] liquid stools that stuck to the anus

Images were captured using a digital camera and the NIS-elements Nikon software package. Fluorescence signals were captured selectively using excitation and emission filters, each of them creating a different color channel. The

Table 2 Characteristics of primary and secondary antibodies

	Host	Dilution	Source	RRID	References
Antigen					
P2X7 receptor	Rabbit	1:200	Merck Millipore (AB5246, lot 2361386)	AB_91773	Evangelinellis et al. (2022), Palombit et al. (2019), Mendes et al. (2023)
nNOS	Sheep	1:2000	Merck Millipore (AB1529, lot 2488802)	AB_90743	Evangelinellis et al. (2022), Palombit et al. (2019)
ChAT	Goat	1:100	Merck Millipore (AB144P, lot 1978747)	AB_2079751	Evangelinellis et al. (2022), Palombit et al. (2019)
PGP9.5	Guinea pig	1:100	Merck Millipore (AB5898, lot 0512018093)	AB_92122	
GFAP	Rabbit	1:400	DAKO (Z0334/lot 00061481)	AB_10013382	Mendes et al. (2023)
Secondary antibodies					
Alexa Fluor 488-conjugated donkey anti-rabbit IgG	Donkey	1:500	Molecular Probes (A21206, lot 1182675)	AB_2535792	Evangelinellis et al. (2022), Palombit et al. (2019), Mendes et al. (2023)
Alexa Fluor 594-conjugated donkey anti-sheep IgG	Donkey	1:100	Molecular Probes (A11016, lot 93D1-1)	AB_2534083	
Alexa Fluor 594-conjugated donkey anti-guinea pig IgG	Donkey	1:200	Molecular Probes (A11076)	AB_141930	

RRID Research Resource Identification Portal https://www.rrids.org/

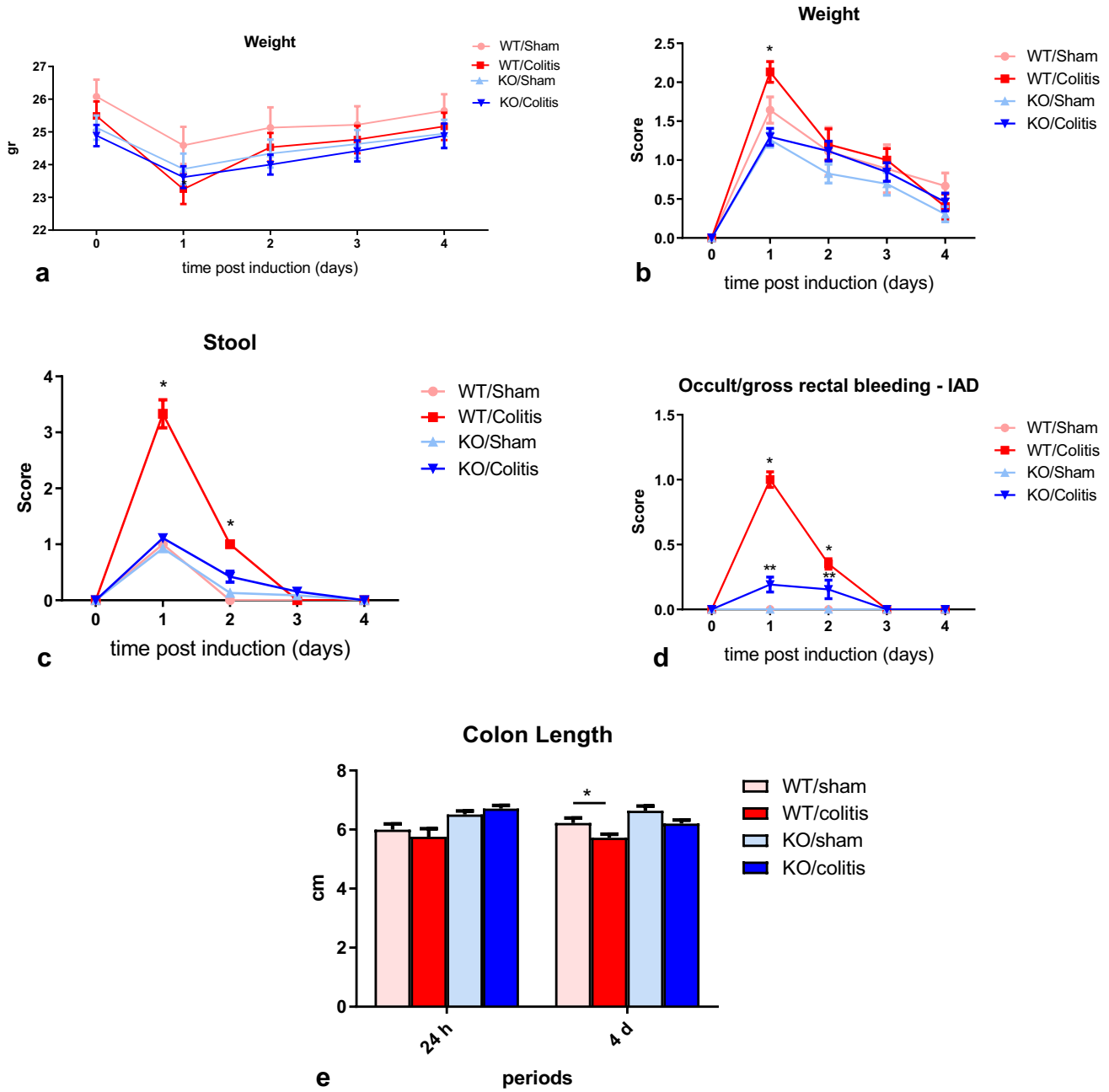

Fig. 1 DAIs of the animals in the WT/sham, WT/colitis, KO/sham, and KO/colitis groups. **a** Weight (g), **b** weight change, **c** stool consistency, **d** occult/gross bleeding, and **e** colon length. A total of 72 animals were used. Data from the 24 h-WT/sham ($n=8$), 24 h-WT/colitis ($n=8$), 24 h-KO/sham ($n=10$), 24 h-KO/colitis ($n=10$), 4 day-WT/sham ($n=8$), 4 day-WT/colitis ($n=8$), 4 day-KO/sham ($n=10$), and 4 day-KO/colitis ($n=10$) groups were evaluated. The data were analyzed by ANOVA and Tukey's multiple comparisons test, as appropriate. $P<0.05$ was considered to indicate statistical significance. $^{*}P<0.05$ for the comparison of the WT/colitis group with the WT/sham group. $^{**}P<0.05$ for the comparison of the KO/colitis group with the KO/sham group. The data are expressed as the means ± standard deviations

RGB images were acquired by a color camera typically with three components that represent red, green, and blue channel intensities. We can display a single-color channel using the tabs located in the bottom-left corner of the image window. Images were collected using processing software and were further processed using Corel Draw software (Evangelinellis et al. 2022).

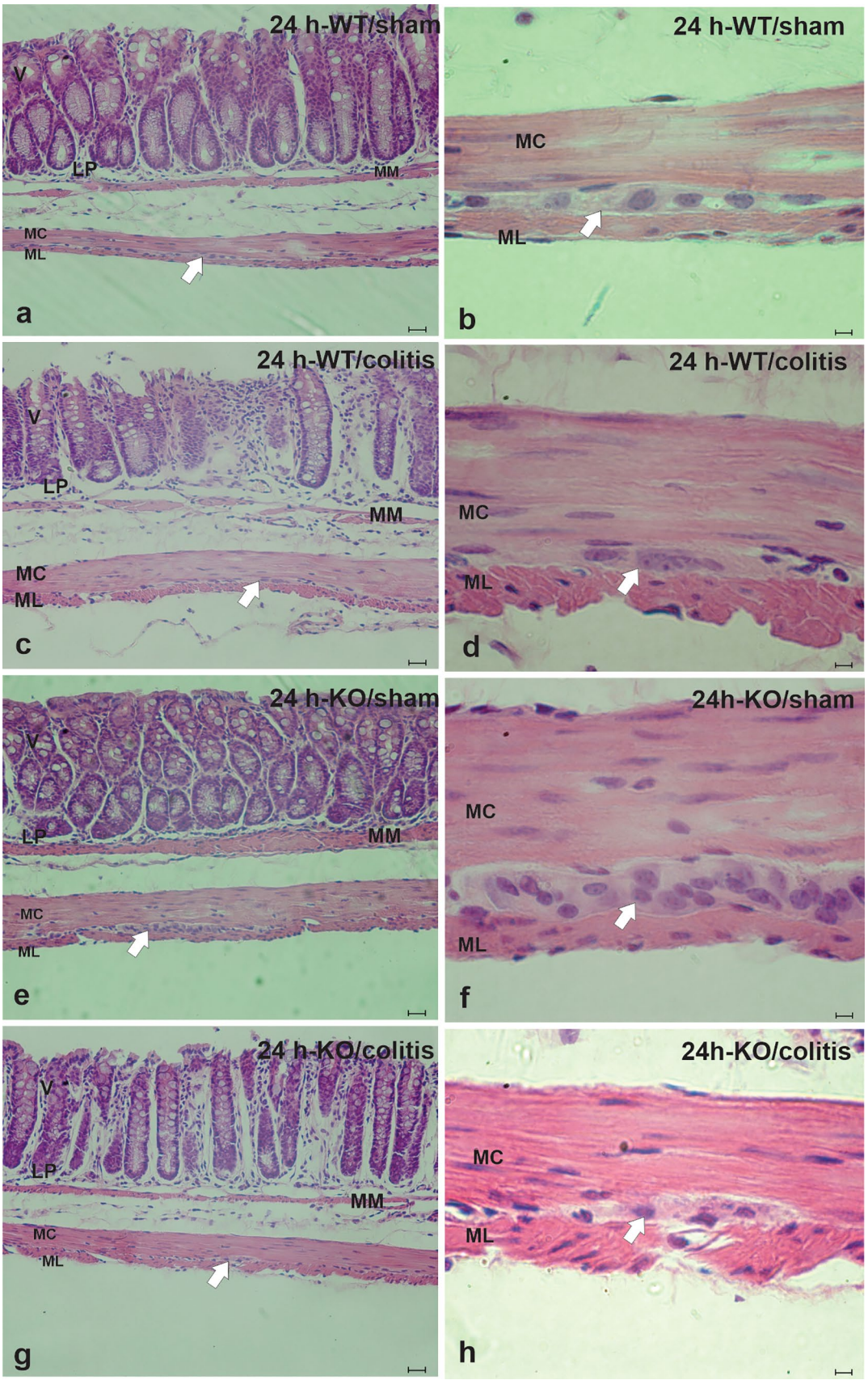
24 h-WT/sham
V
LP
MM
MC
ML
a
24 h-WT/sham
MC
ML
b
24 h-WT/colitis
V
LP
MM
MC
ML
c
24 h-WT/colitis
MC
ML
d
24 h-KO/sham
V
LP
MM
MC
ML
e
24h-KO/sham
MC
ML
f
24 h-KO/colitis
V
LP
MM
MC
ML
g
24h-KO/colitis
MC
ML
h

◂**Fig. 2** Photomicrographs showing H&E-stained sections of the myenteric plexus of the distal colon of the **a**, **b** 24 h-WT/sham, **c**, **d** 24 h-WT/colitis, **e**, **f** 24 h-KO/sham, and **g**, **h** 24 h-KO/colitis groups. Histological images of the 24 h-WT/colitis group showing the appearance of the mucosa, edema, and inflammatory cell infiltration. In the WT/sham and KO groups, the mucosa, circular and longitudinal muscles, and enteric neurons were preserved. The white arrows indicate the myenteric ganglia. *ML* muscular layer, *M* mucosa, *LP* lamina propria, *MM* mucosa muscular, *CM* circular muscle, *LM* longitudinal plexus. Scale bars: 100 µm (**a**, **c**, **e**, **g**); 10 µm (**b**, **d**, **e**, **f**)

Histological analysis

Tissue samples from all the groups were washed with PBS and fixed as described previously (da Silva et al. 2015; Evangenillelis et al. 2022). Distal colon samples were cut into 5-mm sections and stained with hematoxylin–eosin (H&E). Qualitative analysis was performed, and images were taken with a Nikon 80i microscope coupled to a camera with NIS-Elements AR 3.1 software (Nikon).

Quantitative analysis

The number of P2X7 receptor-ir, nNOS-ir, ChAT-ir, PGP9.5-ir, and GFAP-ir neurons per ganglion and the neuronal profile area were measured at ×40 magnification. Cells positive for each antigen in 40 ganglia per animal were counted. A total of 1600 ganglia in the distal colon immunostained for P2X7 receptor, nNOS, PGP9.5, ChAT, or GFAP from the 24 h-WT/sham ($n=5$), 24 h-WT/colitis ($n=5$), 24 h-KO/sham ($n=5$), 24 h-KO/colitis ($n=5$), 4 day-WT/sham ($n=5$), 4 day-WT/colitis ($n=5$), 4 day-KO/sham ($n=5$), and 4 day-KO/colitis ($n=5$) groups were analyzed. A total of 8000 ganglia were analyzed.

The areas (μm^2) of 100 randomly selected nNOS-ir, ChAT-ir, and PGP9.5-ir neurons in preparations from the 24 h-WT/sham ($n=5$), 24 h-WT/colitis ($n=5$), 24 h-KO/sham ($n=5$), 24 h-KO/colitis ($n=5$), 4 day-WT/sham ($n=5$), 4 day-WT/colitis ($n=5$), 4 day-KO/sham ($n=5$), and 4 day-KO/colitis ($n=5$) groups were analyzed as previously described (Evangelinellis et al. 2022).

The data were analyzed by two-way analysis of variance (ANOVA) and Tukey's multiple comparisons test as appropriate using GraphPad 5.0 software (Prism) and are shown as the means ± standard errors of the mean (SEMs). $P<0.05$ was considered to indicate statistical significance.

Results

The DAI of the 24 h-WT/colitis group was higher than those of the 24 h-WT/sham, 24 h-KO/sham, and 24 h-KO/colitis groups, indicating that the former group exhibited weight loss, changes in stool consistency, and occult bleeding. Lower DAI were found for the KO/colitis groups (Fig. 1). No significant difference in colon length was found among the 24 h- and 4 day-KO/sham groups and the 24 h- and 4 day-KO/colitis groups (Fig. 1e).

Histology

Histological analyses showed infiltration of inflammatory cells and edema in the lamina propria and mucosa in the 24 h-WT/colitis and 4 day-WT/colitis groups (Figs. 2 and 3). Edema was observed in the 24 h-KO/colitis group, and the degree of edema in the 4 day-KO/colitis group was similar to that found in the KO/sham group. Microscopic scores revealed ulcerations, edema, and inflammatory cell infiltration in the distal colon in the 24 h-WT/colitis group, but these changes were alleviated in the KO/sham and KO/colitis groups (Table 3).

Immunohistochemistry

The P2X7 receptor was found to be expressed in myenteric neurons in the 24 h-WT/sham, 24 h-WT/colitis, 4 day-WT/sham, and 4 day-WT/colitis groups (Figs. 4, 5, 6, 7, 8). No immunoreactivity was observed in the 24 h- and 4 day-KO/sham and 24 h- and 4 day-KO/colitis groups. The nNOS-ir neurons exhibited a Dogiel type I morphology (Figs. 4, 5) in all the groups, and the ChAT-positive neurons showed Dogiel type I and II morphologies (Figs. 6, 7) in all the groups. As shown in Figs. 8 and 9, PGP9.5 and GFAP labelling was detected in the myenteric ganglia of the 24 h and 4 day groups.

The number of P2X7 receptor-positive neurons per ganglion was reduced by 13.9% and 7% in the 24 h-WT/colitis and 4 day-WT/colitis groups compared to the 24 h-WT/sham and 4 day-WT/sham groups, respectively ($P<0.05$) (Fig. 10a).

The number of nNOS-ir neurons per ganglion was reduced by 32% and 15.7% in the 24 h-WT/colitis and 4 day-WT/colitis groups compared to the 24 h-WT/sham and 4 day-WT/sham groups, respectively ($P<0.05$) (Fig. 10b). Moreover, the number of nNOS-ir neurons/ganglia in the 24 h-KO/colitis group was reduced by 29.7% compared to that in the 24 h-KO/sham group ($P<0.05$) (Fig. 10b). No significant difference was found between the 4 day-KO/sham and 4 day-K/colitis groups.

The number of ChAT-positive neurons per ganglion was decreased by 20.1% and 12.3% in the 24 h-WT/colitis and 4 day-WT/colitis groups compared to the 24 h-WT/sham and 4 day-WT/sham groups, respectively ($P<0.05$) (Fig. 10c).

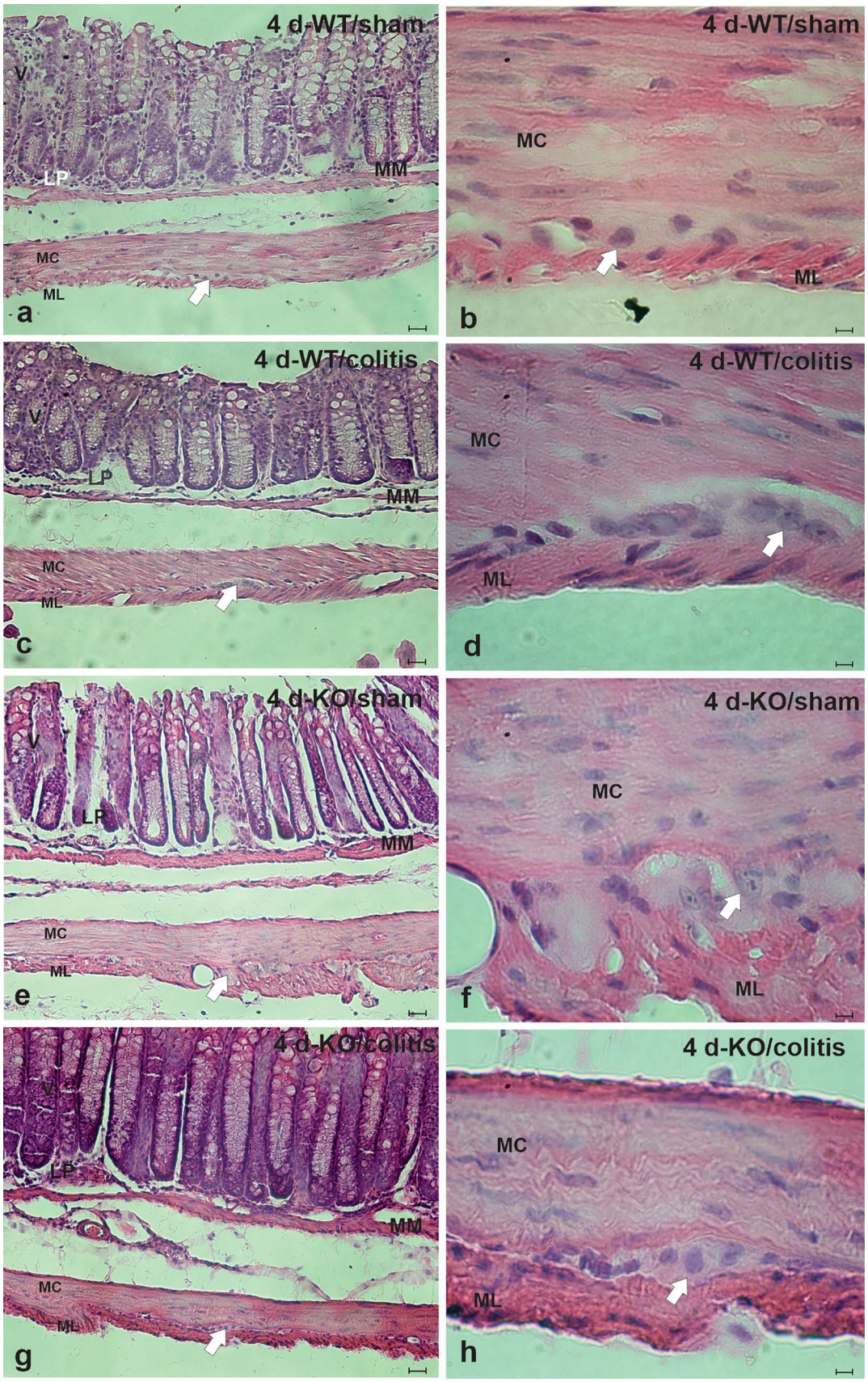
4 d-WT/sham
V
LP
MM
MC
ML
a
4 d-WT/sham
MC
ML
b
4 d-WT/colitis
V
LP
MM
MC
ML
c
4 d-WT/colitis
MC
ML
d
4 d-KO/sham
V
LP
MM
MC
ML
e
4 d-KO/sham
MC
ML
f
4 d-KO/colitis
V
LP
MM
MC
ML
g
4 d-KO/colitis
MC
ML
h

◂**Fig. 3** Photomicrographs showing H&E-stained sections of the myenteric plexus of the distal colon of the **a**, **b** 4 day-WT/sham, **c**, **d** 4 day-WT/colitis, **e**, **f** 4 day-KO/sham, and **g**, **h** 4 day-KO/colitis groups. Histological images showing the appearance of the mucosa; less edema and inflammatory cell infiltration were observed in the WT/colitis group than in the other KO/colitis groups. In the WT/sham and KO/sham groups, the mucosa, circular and longitudinal muscles, and enteric neurons were preserved. The white arrows indicate the myenteric ganglia. *ML* muscular layer, *M* mucosa, *LP* lamina propria, *MM* mucosa muscular, *CM* circular muscle, *LM* longitudinal plexus. Scale bars: 100 µm (**a**, **c**, **e**, **g**); 10 µm (**b**, **d**, **e**, **f**)

Additionally, the number of ChAT-positive neurons per ganglion in the 24 h-KO/colitis group was reduced by 18.3% compared to those in the 24 h-KO/sham group ($P < 0.05$) (Fig. 10c). No significant differences were found between the 4 day-KO/sham and 4 day-KO/colitis groups.

The number of PGP9.5-ir neurons per ganglion was reduced by 13% and 7.6% in the 24 h-WT/colitis and 4 day-WT/colitis groups compared to the 24 h-WT/sham and 4 day-WT/sham groups, respectively ($P < 0.05$) (Fig. 10d). No significant difference was detected among the 24 h- and 4 day-KO/sham and 24 h- and 4 day-KO/colitis groups.

The number of GFAP-positive EGCs per area was decreased by 19.3% in the 24 h-WT/colitis group compared to the 24 h-WT/sham group ($P < 0.05$) and was increased in the 4 day-WT/colitis group compared to the 4 day-WT/sham group ($P < 0.05$) (Fig. 10e). No significant difference was found among the 24 h- and 4 day-KO/sham and 24 h- and 4 day-KO/colitis groups.

The profile area of nNOS-ir neurons (μm^2) was increased by 12.1% and 18.5% in the 4 day-WT/colitis and 4 day-KO/colitis groups compared to the 4 day-WT/sham and 4 day-KO/sham groups, respectively ($P < 0.05$) (Fig. 11a). No significant difference in the profile area was found among the 24 h-WT/sham, 24 h-WT/colitis, 24 h-KO/sham, and 24 h-KO/colitis groups ($P > 0.05$). The size of nNOS-positive neurons ranged from 50 to 1050 μm^2.

The profile area of ChAT-ir neurons was increased by 17.4% and 27.2% in the 4 day-WT/colitis and 4 day-KO/colitis groups compared to the 4 day-WT/sham and 4 day-KO/sham groups, respectively ($P < 0.05$) (Fig. 11b). No significant difference in the profile of ChAT-positive neurons was found among the 24 h-WT/sham, 24 h-WT/colitis, 24 h-KO/sham, and 24 h-KO/colitis groups ($P > 0.05$). The size of ChAT-ir neurons ranged from 50 to 950 μm^2.

The area of PGP9.5-ir neurons was increased by 14.7% and 19.7% in the 4 day-KO/colitis and 4 day-KO/colitis groups compared to the 4 day-KO/sham and 4 day-KO/sham groups, respectively ($P < 0.05$). No significant difference in the profile of PGP9.5-ir neurons was found among the 24 h-WT/sham and 24 h-WT/colitis groups ($P > 0.05$) (Fig. 11c). The size of PGP9.5-ir neurons ranged from 50 to 900 μm^2.

Discussion

The present study showed the effects on the myenteric plexus of WT and P2X7 receptor-KO mice at 24 h and 4 days after the induction of experimental ulcerative colitis. The numbers of nNOS-ir, ChAT-ir, and PGP9.5-ir myenteric plexus and GFAP-ir glial cells were decreased in the 24 h- and 4 day-WT/colitis groups, and no change was found in the 4 day-KO/colitis group. In addition, the distal colon of 24 h-WT/colitis group exhibited lesions, hyperemia, and inflammation, whereas the distal colon of the 4 day-KO/colitis group showed no macroscopic changes. The DAIs of the 24 h-WT/colitis and 4 day-WT/colitis groups showed alterations in weight, stool consistency, and blood in the stool, and these parameters were improved in the KO/colitis groups.

TNBS has been widely used to establish models of IBDs in both rats and mice (Matsuura et al. 2005; da Silva et al. 2015; Chen et al. 2018; Zhou et al. 2018; Evangelinellis et al. 2022). In the present work, macroscopic differences in the target tissue reflecting tissue damage caused by the inflammatory process were not detected in the 4 day groups using this scale. According to the literature, hyperemia, the presence of ulcerations, and increases in lamina propria size and edema area were observed 24 h after colitis induction (Linden et al. 2005; da Silva et al. 2015; Evangelinellis et al. 2022). Among the 24 h groups, only the 24 h-WT/colitis group showed macroscopic changes, and hyperemia in the mucosa of the distal colon was observed in this group but was alleviated over the following days. Tissues collected 4 days after colitis induction did not show any macroscopic changes. According to the DAI analysis, diarrhea, bleeding, and weight loss were mainly observed in the animals in the 24 h-WT/colitis and 4 day-WT/colitis groups. These changes were observed to a lesser extent in the WT/sham, KO/sham, and KO/colitis groups because only the feces and weight of these groups were altered.

Alterations in the density of the myenteric plexus have been widely studied in different models, such as experimental ulcerative colitis (Linden et al. 2005; Gulbransen et al. 2012; da Silva et al. 2015; Evangelinellis et al. 2022). After the induction of intestinal inflammation, decreases in the numbers of enteric neurons expressing P2X7, ChAT, nNOS, and PGP9.5 were observed in the 24 h-WT/colitis and 4 day-WT/colitis groups. The reduction in the number of GFAP-ir glia detected in the 24 h-WT/colitis group is consistent with

Table 3 Macroscopic and microscopic scores of the distal colon in the WT/sham, WT/colitis, KO/sham, and KO/colitis groups

Variables	24 h-WT/sham	24 h-WT/colitis	24 h-KO/sham	24 h-KO/colitis	4 day-WT/sham	4 day-WT/colitis	4 day-KO/sham	4 day-KO/colitis
Macroscopic score	0	1.5 ± 0.1	0	0	0	0	0	0
Microscopic score								
Ulcerations	0	0	0	0	0	0	0	0
Edema (submucosal)	0	2.0 ± 0.2	0	0.9 ± 0.2	0	1.9 ± 0.1	0	0
Inflammatory cell infiltration	0	3.0 ± 0.1	0	1.0 ± 0.1	0	3.0 ± 0.2	0	0

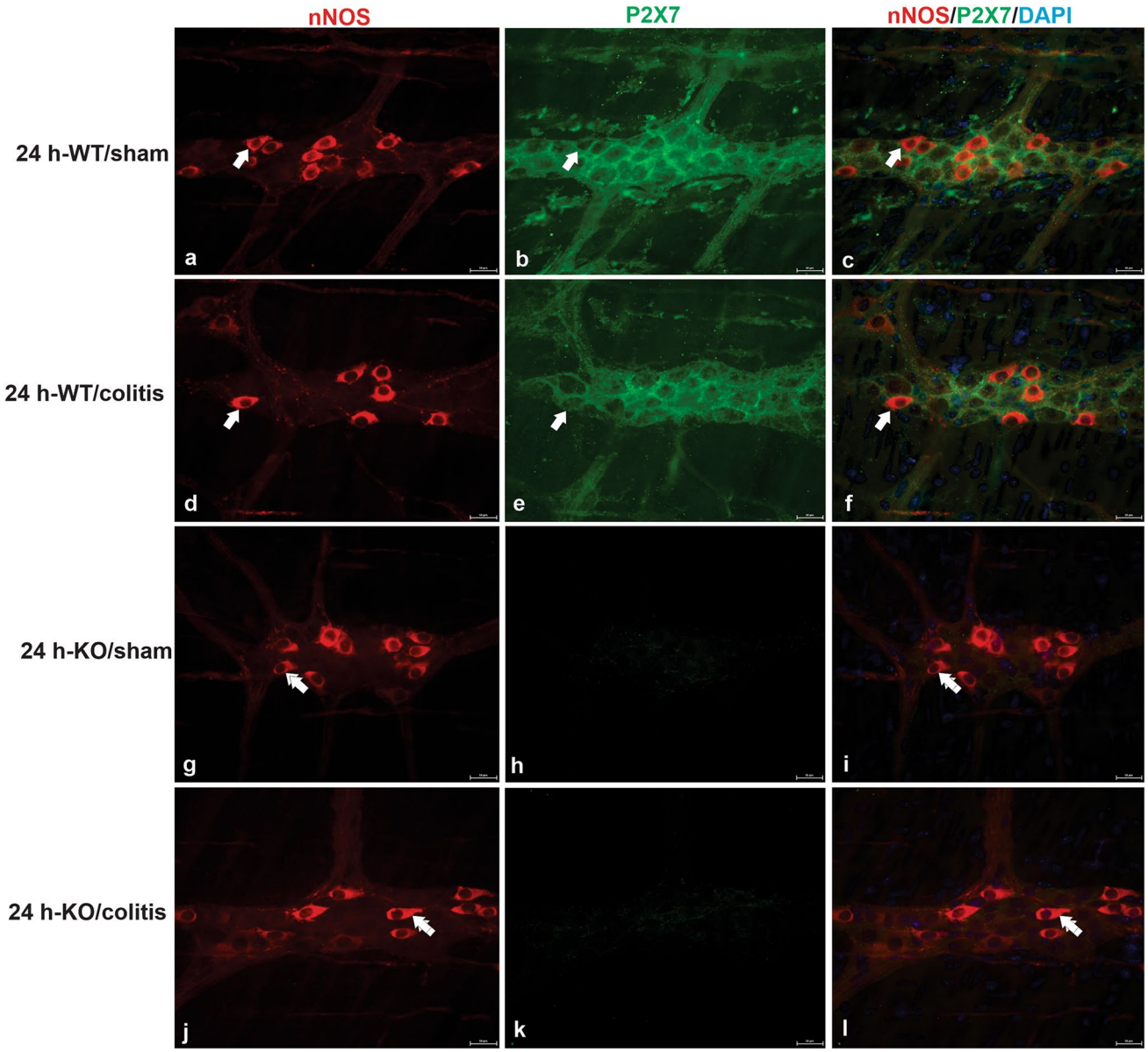

Fig. 4 Double labelling of **a**, **d** nNOS and **b**, **e** P2X7 receptor in neurons in the myenteric plexus of the distal colon of the **a**–**c** 24 h-WT/sham and **d**–**f** 24 h-WT/colitis groups. **c**, **f** Overlap of nNOS (red; **a**, **d**) and P2X7 receptor (green; **b**, **e**). **c**, **f** DAPI (blue) staining of nuclei. **i**, **l** nNOS staining (red; **g**, **j**) in 24 h KO/sham and 24 h-KO/colitis mice. **h**, **k** Lack of staining of the P2X7 receptor in the 24 h-KO/sham and 24 h-KO/colitis groups. **i**, **l** DAPI (blue) staining of nuclei. The single arrows indicate double-labelled neurons. Scale bars = 50 µm

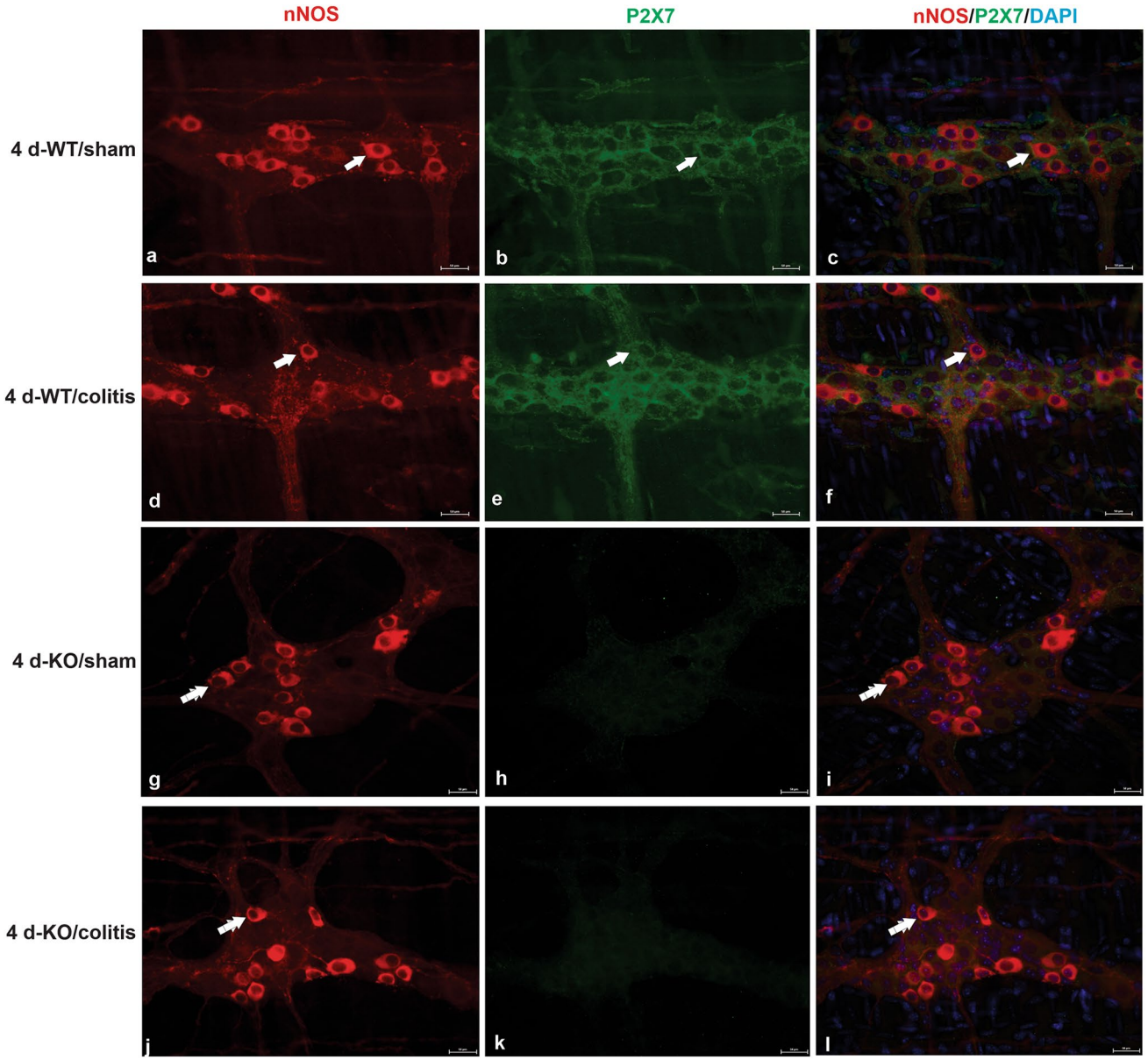

Fig. 5 Double labelling of **a**, **d** nNOS and **b**, **e** P2X7 receptor in neurons in the myenteric plexus of the distal colon of the **a**–**c** 4 day-WT/sham and **d**–**f** 4 day-WT/colitis groups. **c**, **f** Overlap of nNOS (red; **a**, **d**) and P2X7 receptor (green; **b**, **e**). **c**, **f** DAPI (blue) staining of nuclei. **i**, **l** nNOS staining (red; **g**, **j**) in 4 day-KO/sham and 4 day-KO/colitis mice. **h**, **k** Lack of staining of the P2X7 receptor in the 4 day-KO/sham and 4 day-KO/colitis groups. **i**, **l** DAPI (blue) staining of nuclei. The single arrows indicate double-labelled neurons. Scale bars = 50 µm

the findings reported in the literature (Linden et al. 2005; Gulbransen et al. 2012; da Silva et al. 2015; Evangelinellis et al. 2022). It is possible that the decrease in the number of these neurons was due to activation of pathways other than the P2X7 receptor pathway, such as the IL-1β, TNFα, IL-7, and caspase-independent apoptosis pathways (Kermarrec et al. 2019). However, the percent decrease in the number of ChAT-ir and nNOS-ir neurons was smaller in the 24 h-KO/colitis group than in the 24 h-WT/colitis group, indicating that loss of the P2X7 receptor may have a mild protective effect. No significant difference in the PGP9.5-ir, nNOS-ir, and ChAT-ir neurons was found among the 24 h- and 4 day-KO/sham and 24 h- and 4 day-KO/colitis groups, demonstrating that inhibiting the action of the P2X7 receptor may protect against neuronal death (Peng et al. 2009; Palombit et al. 2019; Souza et al. 2020; Magalhães and

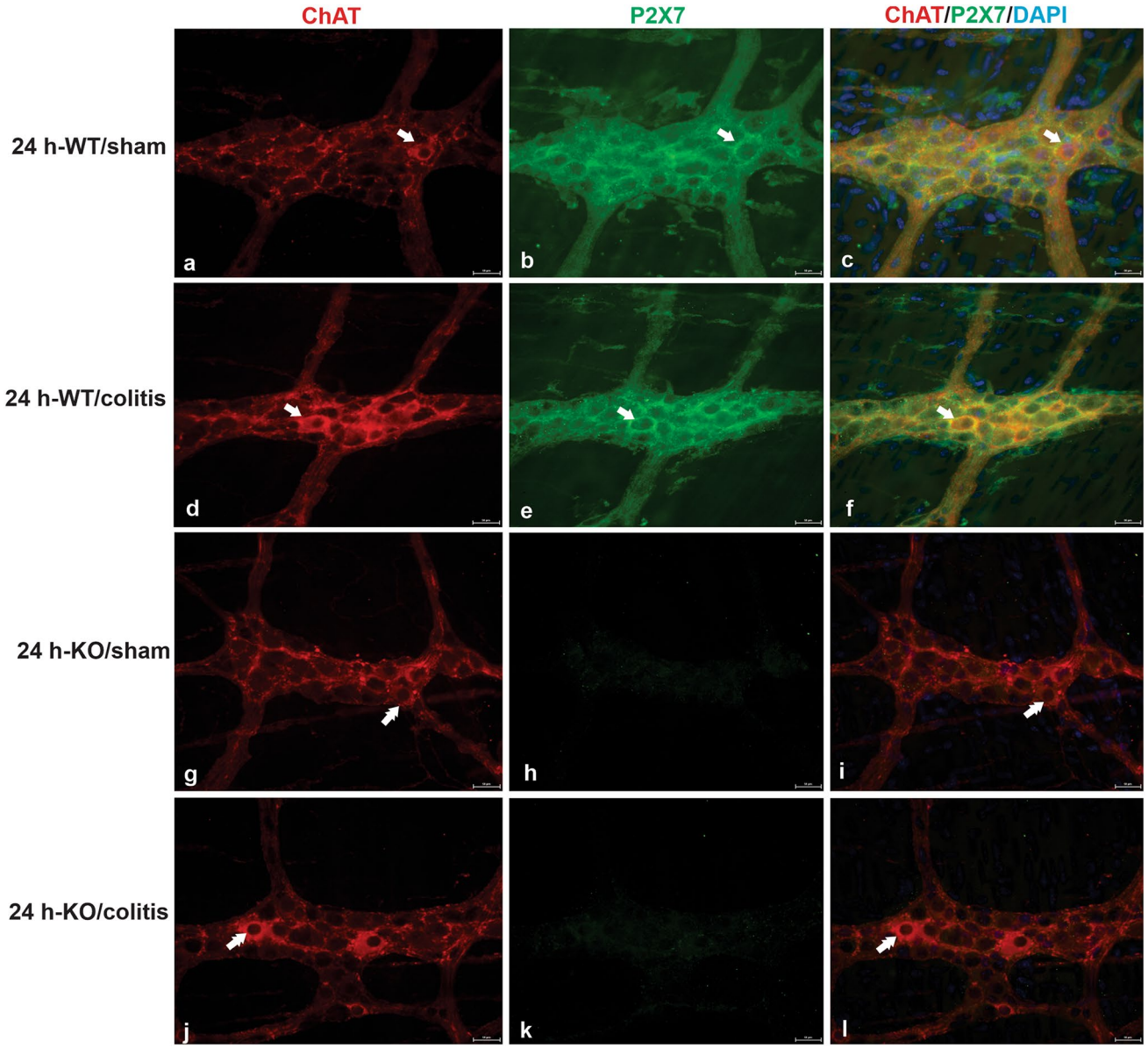

Fig. 6 Double labelling of **a**, **d** ChAT and **b**, **e** P2X7 receptor in neurons in the myenteric plexus of the distal colon of the **a**–**c** 24 h-WT/sham and **d**–**f** 24 h-WT/colitis groups. **c**, **f** Overlap of nNOS (red; **a**, **d**) and P2X7 receptor (green; **b**, **e**). **c**, **f** DAPI (blue) staining of nuclei. **i**, **l** ChAT staining (red; **g**, **j**) in the 24 h-KO/sham and 24 h-KO/colitis groups. **h**, **k** Lack of staining of the P2X7 receptor in the 24 h-KO/sham and 24 h-KO/colitis groups. **i**, **l** DAPI (blue) staining of nuclei. The single arrows indicate double-labelled neurons. Scale bars = 50 µm

Castelucci 2021; Evangelinellis et al. 2022). According to the literature, P2X7 receptor blockade exerts a neuroprotective effect, and P2X7 knockout may increase the expression of the anti-inflammatory factors IL-10 and transforming growth factor-β1 (TGF-β1) and thus control inflammation (Hofman et al. 2015; Figliuolo et al. 2017; Magalhães and Castelucci 2021).

EGCs regulate permeability, neuronal activity (through either intrinsic or extrinsic innervation), immune functions, absorption, motility, vascular tone, and secretion (Gulbransen and Sharkey 2012). Owing to their functional plasticity, EGCs have a very important homeostatic function, and understanding the roles of these cells is essential for identifying new therapeutic targets (Ochoa-Cortes et al.

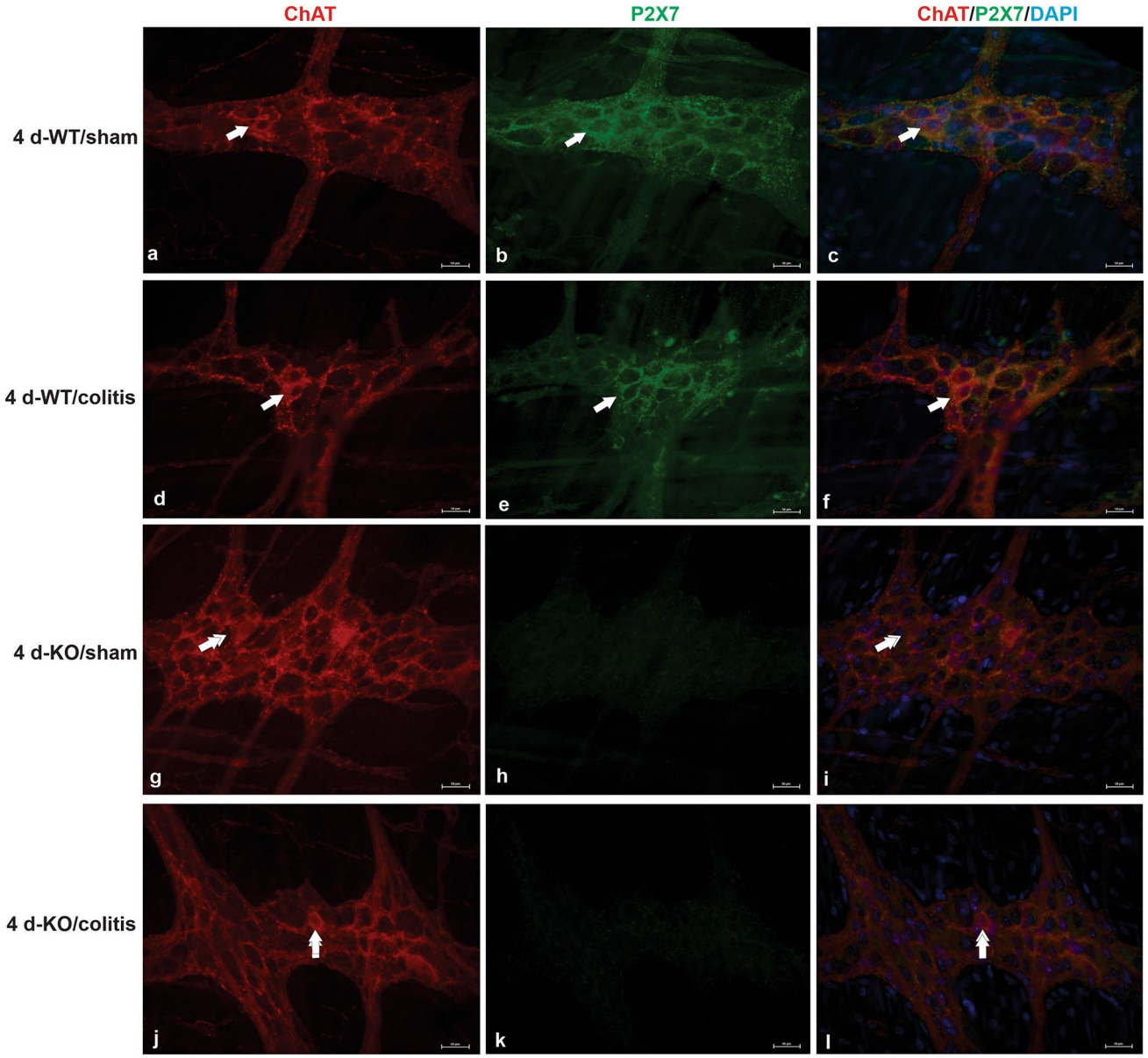

Fig. 7 Double labelling of **a**, **d** ChAT and **b**, **e** P2X7 receptor in neurons in the myenteric plexus of the distal colon of the **a**–**c** 4 day-WT/sham and **d**–**f** 4 day-WT/colitis groups. **c**, **f** Overlap of ChAT (red; **a**, **d**) and P2X7 receptor (green; **b**, **e**). **c**, **f** DAPI (blue) staining of nuclei. **i**, **l** ChAT staining (red; **g**, **j**) in the 4 day-KO/sham and 4 day-KO/colitis groups. **h**, **k** Lack of staining of the P2X7 receptor in the 4 day-KO/sham and 4 day-KO/colitis groups. **i**, **l** DAPI (blue) staining of nuclei. The single arrows indicate double-labelled neurons. Scale bars = 50 µm

2016). The heterogeneity and plasticity (functional and chemical) of EGCs must be considered in the pathogenesis and etiology of gastrointestinal diseases (Valès et al. 2018).

Our work revealed a decrease in the density of EGCs expressing GFAP in the 24 h-WT/colitis group. The opposite changes were observed in the 4 day-WT/colitis group because the density of GFAP-positive glia was increased in this group. EGCs exert different effects against gastrointestinal disorders, and elucidating these effects will help provide new treatments for human diseases (Gulbransen and Christofi 2018). EGCs perform a role in cell proliferation and differentiation to maintain homeostasis (Gulbransen and Sharkey 2012; Coelho-Aguiar et al. 2015; Mendes et al.

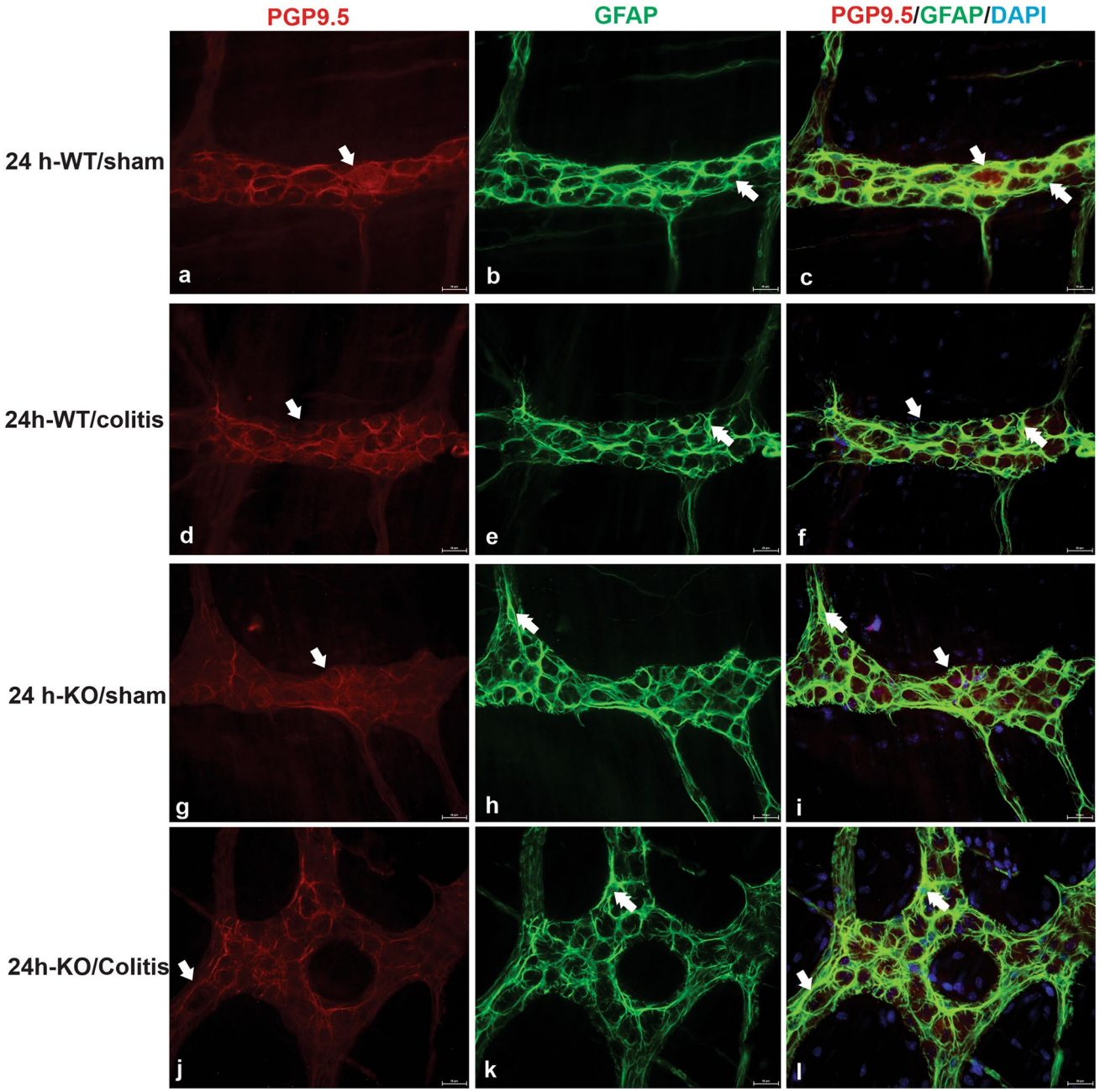

Fig. 8 Double labelling of **a**, **d** PGP9.5 (pan neuronal) and **b**, **e** GFAP (a glial marker) in neurons in the myenteric plexus of the distal colon of the **a**–**c** 24 h-WT/sham and **d**–**f** 24 h-WT/colitis groups. **c**, **f** Merged image of PGP9.5 (red; **a**, **d**) and GFAP (green; **b**, **e**) staining. **c**, **f** DAPI (blue) staining of nuclei. **i**, **l** PGP9.5 (red; **g**, **j**) and GFAP (green, **h**, **k**) staining in the 24 h-KO/sham and 24 h-KO/colitis groups. **i**, **l** DAPI (blue) staining of nuclei. The single arrows indicate PGP9.5 staining, and the double arrows indicate glial cell staining. Scale bars = 50 µm

2015, 2019; Gulbransen and Christofi 2018; Li et al. 2018; Costa et al. 2019).

An increase in the area of nNOS-ir, ChAT-ir, and PGP9.5-ir neurons was only found in the 4 day-WT/colitis group. Changes in the cell area are closely linked to cell necrosis, which is characterized by increases in chromatin aggregation and cell volume that lead to cell content leakage and may cause damage to adjacent cells (Berghe et al. 2014; Galluzzi et al. 2014). Changes in the cell area can also result from apoptosis, in which loss of adherence to the extracellular matrix and neighboring cells is caused by cell retraction,

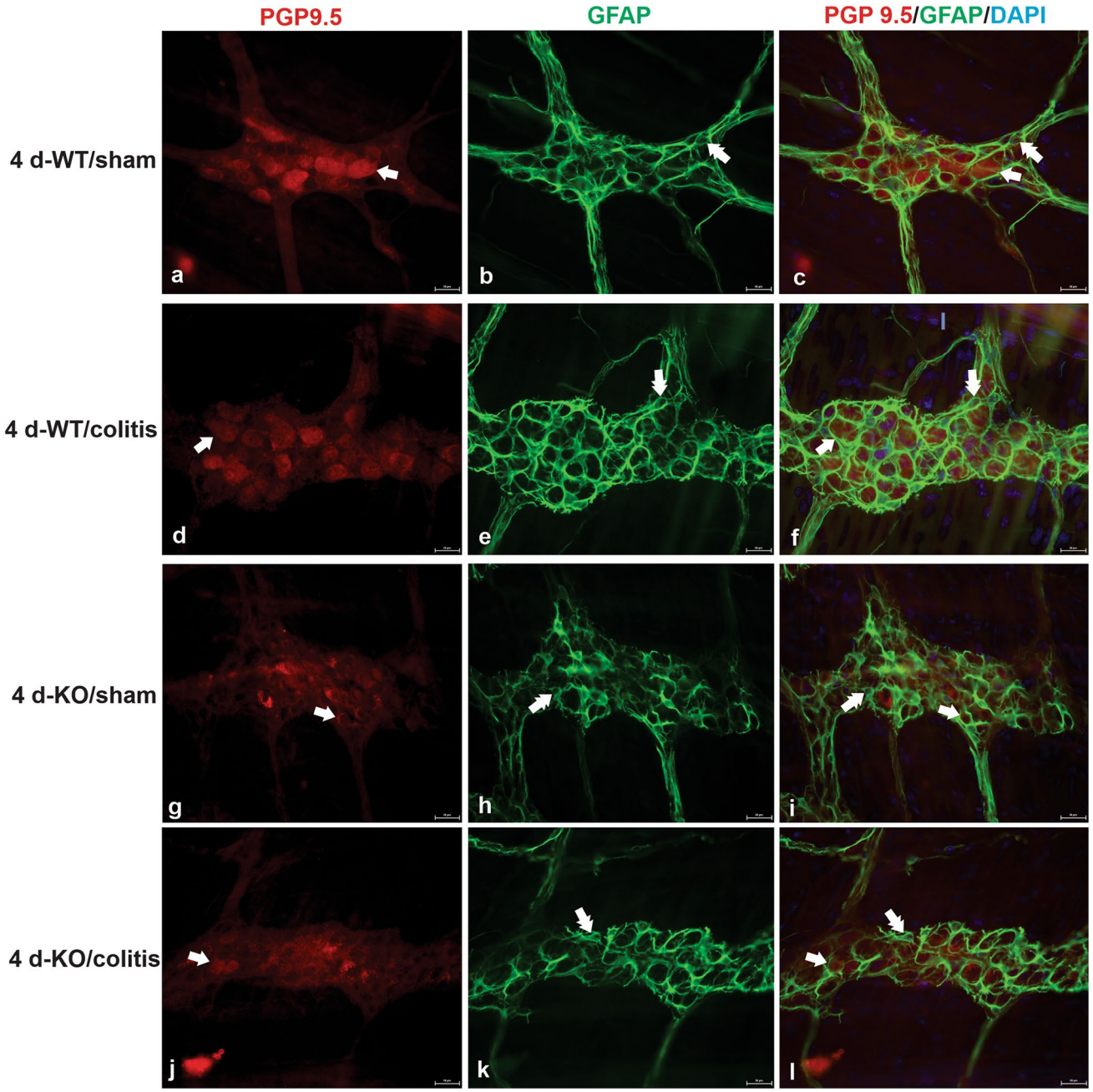

Fig. 9 Double labelling of **a**, **d** PGP9.5 (pan neuronal) and **b**, **e** GFAP (glial marker) in neurons in the myenteric plexus of the distal colon of the **a**–**c** 4 day-WT/sham and **d**–**f** 4 day-WT/colitis groups. **c**, **f** Merged image of PGP9.5 (red; **a**, **d**) and GFAP (green; **b**, **e**) staining. **c**, **f** DAPI (blue) staining of nuclei. **i**, **l** PGP9.5 (red; **g**, **j**) and GFAP (green, **h**, **k**) staining in the 4 day-KO/sham and 4 day-KO/colitis groups. **i**, **l** DAPI (blue) staining of nuclei. The single arrows indicate PGP9.5 staining, and the double arrows indicate glial cell staining. Scale bars = 50 µm

causing a decrease in the cell area (Ziegler and Groscurth 2004; Kulkarni et al. 2017).

The effects of pharmacological or genetic blockade of the P2X7 receptor have been widely studied and have been found to be positive in several human diseases. Cell death via the P2X7 receptor and the release of cytokines play a fundamental role in pathophysiology; however, further studies of the molecular mechanisms of the receptor and their effects are needed to aid the development of treatments for human diseases (Kopp et al. 2019). Following activation of the P2X7 receptor, the influx of Ca^{2+} ions increases with activation of the caspase pathway, which

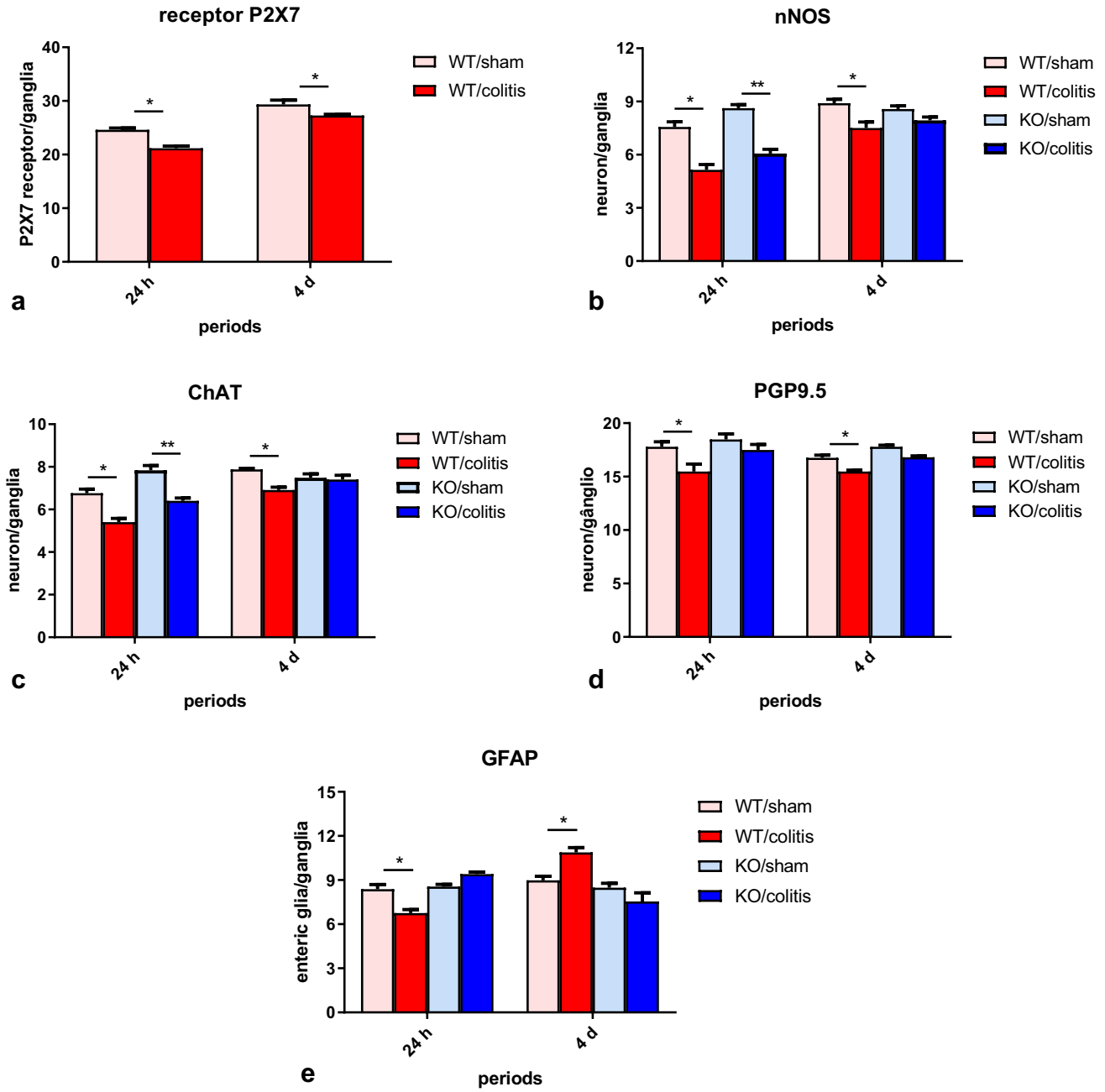

Fig. 10 Number of neurons expressing **a** P2X7 receptor, **b** nNOS, **c** ChAT, and **d** PGP9.5, and **e** GFAP-expressing glial cells per ganglion in the myenteric plexus of the distal colon of mice in the WT/sham, WT/colitis, KO/sham, and KO/colitis groups at 24 h and 4 days. The neurons in 40 ganglia from each animal were counted. The numbers of P2X7 receptor-ir, nNOS-ir, ChAT-ir, and PGP9.5-ir neurons and GFAP-ir glial cells per 200 ganglia were analyzed for each group. The data were analyzed by ANOVA and Tukey's multiple comparisons test, as appropriate. $P < 0.05$ was considered to indicate statistical significance. *$P < 0.05$ for the comparison of the WT/colitis group with the WT/sham group. **$P < 0.05$ for the comparison of the KO/colitis group with the KO/sham group. The data are expressed as the means ± standard deviations

causes the release of active inflammatory mediators, such as IL-1β (Kahlenberg 2022), and thus contributes to an even more severe inflammatory response (Mehta et al. 2014). The P2X7 receptor causes apoptosis or necrosis to neurons after injury (Di Virgilio et al. 2017; Franke and Illes 2006).

This work is important because it demonstrates that the P2X7 receptor can be an important therapeutic target in

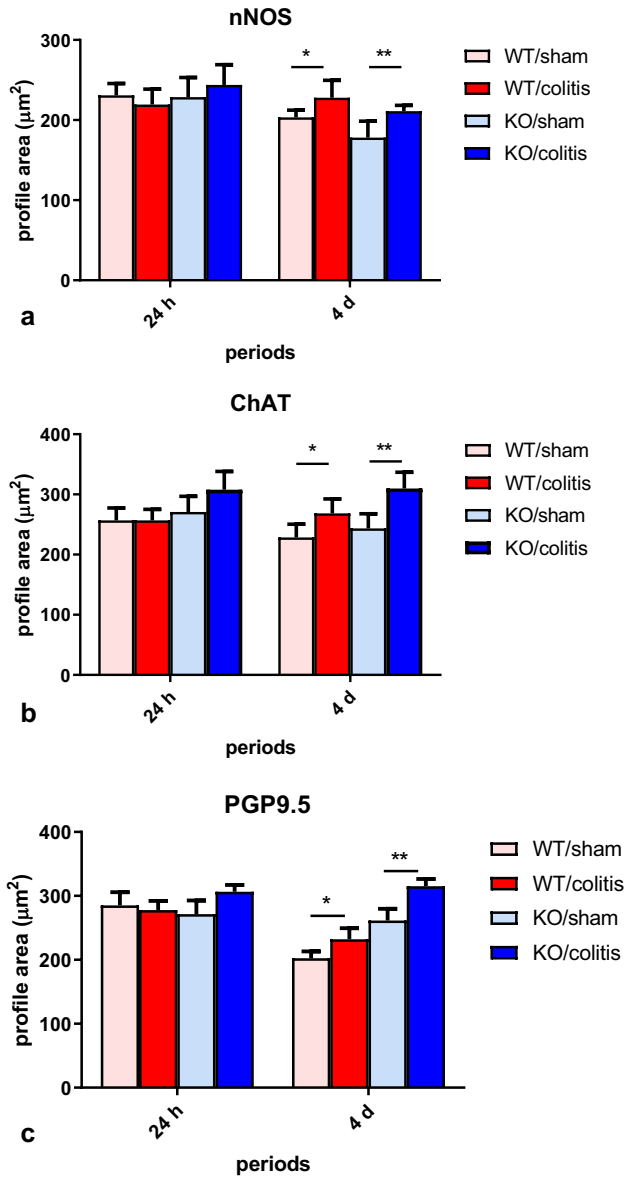

Fig. 11 Areas (μm^2) of **a** nNOS-ir, **b** ChAT-ir, and **c** PGP9.5-ir neurons in the myenteric plexus of the distal colon of mice in the WT/sham, WT/colitis, KO/sham, and KO/colitis groups at 24 h and 4 days. The perikaryal areas (μm^2) of 100 neurons from each animal were measured. A total of 500 neurons positive for nNOS, ChAT, and PGP9.5 were analyzed per group. The data were analyzed by ANOVA and Tukey's multiple comparisons test, as appropriate. $P < 0.05$ was considered to indicate statistical significance. *$P < 0.05$ for the comparison of the WT/colitis group with the WT/sham group. **$P < 0.05$ for the comparison of the KO/colitis group with the KO/sham group. The data are expressed as the means ± standard deviations

inflammation that affects enteric neurons and EGCs in the digestive tract.

Author contributions FAM performed the experiments, analyzed the results, and prepared figures. RFS helped with the experiments and care of animals. VF helped with injection of TNBS and care of animals. RC-S performed experimental design and critical analysis of the results. PC performed experimental design, critical analysis, and wrote the main manuscript text. All authors reviewed the manuscript.

Funding This study was supported by the Foundation São Paulo Research (FAPESP, grant numbers 2014/25927-2 and 2018/07862-1), the Coordenação de Aperfeiçoamento de Pessoal de Nível Superior (CAPES), and the Conselho Nacional de Desenvolvimento Científico e Tecnológico (CNPq).

Data availability Data will be made available upon reasonable request.

Declarations

Conflict of interest The authors declare no conflicts of interest.

References

Abbracchio MP, Burnstock G, Verkhratsky A, Zimmermann H (2009) Purinergic signalling in the nervous system: an overview. Trends Neurosci 32:19–29. https://doi.org/10.1016/j.tins.2008.10.001

Aniwan S, Park SH, Loftus EV (2017) Epidemiology, natural history, and risk stratification of Crohn's disease. Gastroenterol Clin North Am 46:463–480. https://doi.org/10.1016/j.gtc.2017.05.003

Antonioli L, Colucci R, Pellegrini C et al (2013) The role of purinergic pathways in the pathophysiology of gut diseases: pharmacological modulation and potential therapeutic applications. Pharmacol Ther 139:157–188. https://doi.org/10.1016/j.pharmthera.2013.04.002

Antonioli L, Giron MC, Colucci R et al (2014) Involvement of the P2X7 purinergic receptor in colonic motor dysfunction associated with bowel inflammation in rats. PLoS ONE 9:1–20. https://doi.org/10.1371/journal.pone.0116253

Bassotti G, Villanacci V, Fisogni S et al (2007) Enteric glial cells and their role in gastrointestinal motor abnormalities: introducing the neuro-gliopathies. World J Gastroenterol 13:4035–4041. https://doi.org/10.3748/wjg.v13.i30.4035

Bell CJ, Gall DG, Wallace JL (1995) Disruption of colonic electrolyte transport in experimental colitis. American Journal of Physiology-Gastrointestinal and Liver Physiology 268 (4):G622–G630

Berghe T Vanden, Linkermann A, Jouan-Lanhouet S, et al (2014) Regulated necrosis: The expanding network of non-apoptotic cell death pathways. Nat Rev Mol Cell Biol 15:135–147. https://doi.org/10.1038/nrm3737

Chen G, Ran X, Li B et al (2018) Sodium butyrate inhibits inflammation and maintains epithelium barrier integrity in a TNBS-induced inflammatory bowel disease mice model. EBioMedicine 30:317–325. https://doi.org/10.1016/j.ebiom.2018.03.030

Cook TA, Brading AF, Mortensen NJMC (2000) Abnormal contractile properties of rectal smooth muscle in chronic ulcerative colitis. Aliment Pharmacol Ther 14:1287–1294. https://doi.org/10.1046/j.1365-2036.2000.00819.x

Costa DVS, Bon-Frauches AC, Silva AMHP et al (2019) 5-Fluorouracil induces enteric neuron death and glial activation during intestinal mucositis via a S100B-RAGE-NFκB-dependent pathway. Sci Rep 9:655. https://doi.org/10.1038/s41598-018-36878-z

da Silva MV, Marosti AR, Mendes CE et al (2015) Differential effects of experimental ulcerative colitis on P2X7 receptor expression

in enteric neurons. Histochem Cell Biol. https://doi.org/10.1007/s00418-014-1270-6
da Silva MV, Marosti AR, Mendes CE et al (2017) Submucosal neurons and enteric glial cells expressing the P2X7 receptor in rat experimental colitis. Acta Histochem. https://doi.org/10.1016/j.acthis.2017.05.001
de Coelho-Aguiar J M, Bon-Frauches AC, Gomes ALT et al (2015) The enteric glia: identity and functions. Glia 63:921–935. https://doi.org/10.1002/glia.22795
Di Virgilio F, Dal Ben D, Sarti AC, Giuliani AL, Falzoni S (2017) The P2X7 receptor in infection and inflammation. Immunity 47:15–31. https://doi.org/10.1016/j.immuni.2017.06.020
Erdogan B, Isiksoy S, Dundar E, Pasaoglu O, Bal C (2003) The effects of sodium phosphate and polyethylene glycol-electrolyte bowel preparation solutions on 2,4,6-trinitrobenzenesulfonic acid-induced colitis in the rat. Experimental and Toxicologic Pathology 55 (2–3):213–220. https://doi.org/10.1078/0940-2993-00318
Evangelinellis MM, Souza RF, Mendes CE, Castelucci P (2022) Effects of a P2X7 receptor antagonist on myenteric neurons in the distal colon of an experimental rat model of ulcerative colitis. Histochem Cell Biol 157:65–81. https://doi.org/10.1007/s00418-021-02039-z
Fabia R, Ar'rajab A, Johansson ML et al (1993) The effect of exogenous administration of *Lactobacillus reuteri* r2LC and oat fiber on acetic acid-induced colitis in the rat. Scand J Gastroenterol 28:155–162. https://doi.org/10.3109/00365529309096063
Ferri GL, Probert L, Cocchia D et al (1982) Evidence for the presence of S-100 protein in the glial component of the human enteric nervous system. Nature 297:409–410. https://doi.org/10.1038/297409a0
Figliuolo VR, Savio LEB, Safya H et al (2017) P2X7 receptor promotes intestinal inflammation in chemically induced colitis and triggers death of mucosal regulatory T cells. Biochim Biophys Acta Mol Basis Dis 1863:1183–1194. https://doi.org/10.1016/j.bbadis.2017.03.004
Franke H, Illes P (2006) Involvement of P2 receptors in the growth and survival of neurons in the CNS. Pharmacol Ther 109:297–324. https://doi.org/10.1016/j.pharmthera.2005.06.002
Furness JB (2006) The enteric nervous system. Blackwell, Wiley
Furness JB (2012) The enteric nervous system and neurogastroenterology. Nat Rev Gastroenterol Hepatol 9:286–294. https://doi.org/10.1038/nrgastro.2012.32
Galluzzi L, Kepp O, Krautwald S et al (2014) Molecular mechanisms of regulated necrosis. Semin Cell Dev Biol 35:24–32. https://doi.org/10.1016/j.semcdb.2014.02.006
Gulbransen BD, Christofi FL (2018) Are we close to targeting enteric glia in gastrointestinal diseases and motility disorders? Gastroenterology 155:245–251. https://doi.org/10.1053/j.gastro.2018.06.050
Gulbransen BD, Sharkey KA (2012) Novel functional roles for enteric glia in the gastrointestinal tract. Nat Rev Gastroenterol Hepatol 9:625–632. https://doi.org/10.1038/nrgastro.2012.138
Gulbransen BD, Bashashati M, Hirota SA et al (2012) Activation of neuronal P2X7 receptor-pannexin-1 mediates death of enteric neurons during colitis. Nat Med 18:600–604. https://doi.org/10.1038/nm.2679
Hofman P, Cherfils-Vicini J, Bazin M et al (2015) Genetic and pharmacological inactivation of the purinergic P2RX7 receptor dampens inflammation but increases tumor incidence in a mouse model of colitis-associated cancer. Cancer Res 75:835–845. https://doi.org/10.1158/0008-5472.CAN-14-1778
Hu HZ, Gao N, Lin Z et al (2001) P2X7 receptors in the enteric nervous system of guinea-pig small intestine. J Comparat Neurol 440:299–310. https://doi.org/10.1002/cne.1387
Kahlenberg JM, Dubyak GR (2022) Mechanisms of caspase-1 activation by P2X7 receptor-mediated K+ release. Am J Physiol Cell Physiol 44106:1100–1108
Jessen K, Mirsky R (1980) Glial cells in the enteric nervous system contain glial fibrillary acidic protein. Nature 286:736–737
Kappelman MD, Rifas-Shiman SL, Kleinman K et al (2007) The prevalence and geographic distribution of Crohn's disease and ulcerative colitis in the United States. Clin Gastroenterol Hepatol 5:1424–1429. https://doi.org/10.1016/j.cgh.2007.07.012
Kermarrec L, Durand T, Gonzales J et al (2019) Rat enteric glial cells express novel isoforms of interleukine-7 regulated during inflammation. Neurogastroenterol Motil 31:10–14. https://doi.org/10.1111/nmo.13467
Kopp R, Krautloher A, Ramírez-Fernández A, Nicke A (2019) P2X7 interactions and signaling—making head or tail of it. Front Mol Neurosci 12:1–25. https://doi.org/10.3389/fnmol.2019.00183
Kulkarni S, Micci MA, Leser J et al (2017) Adult enteric nervous system in health is maintained by a dynamic balance between neuronal apoptosis and neurogenesis. Proc Natl Acad Sci USA 114:E3709–E3718. https://doi.org/10.1073/pnas.1619406114
Li Y, Ge Y, Zhu W et al (2018) Increased enteric glial cells in proximal margin of resection is associated with postoperative recurrence of Crohn's disease. J Gastroenterol Hepatol 33:638–644. https://doi.org/10.1111/jgh.13973
Linden DR, Couvrette JM, Ciolino A et al (2005) Indiscriminate loss of myenteric neurones in the TNBS-inflamed guinea-pig distal colon. Neurogastroenterol Motil 17:751–760. https://doi.org/10.1111/j.1365-2982.2005.00703.x
Magalhães HIR, Castelucci P (2021) Enteric nervous system and inflammatory bowel diseases: correlated impacts and therapeutic approaches through the P2X7 receptor. World J Gastroenterol 27:7909–7924
Matsuura M, Okazaki K, Nishio A et al (2005) Therapeutic effects of rectal administration of basic fibroblast growth factor on experimental murine colitis. Gastroenterology 128:975–986. https://doi.org/10.1053/j.gastro.2005.01.006
Mehta N, Kaur M, Singh M et al (2014) Purinergic receptor P2X7: a novel target for anti-inflammatory therapy. Bioorg Med Chem 22:54–88. https://doi.org/10.1016/j.bmc.2013.10.054
Mendes CE, Palombit K, Vieira C et al (2015) The effect of ischemia and reperfusion on enteric glial cells and contractile activity in the ileum. Dig Dis Sci. https://doi.org/10.1007/s10620-015-3663-3
Mendes CE, Palombit K, Tavares-de-Lima W, Castelucci P (2019) Enteric glial cells immunoreactive for P2X7 receptor are affected in the ileum following ischemia and reperfusion. Acta Histochem. https://doi.org/10.1016/j.acthis.2019.06.001
Mendes CE, Palombit K, Alves Pereira TT et al (2023) Effects of probenecid and brilliant blue G on rat enteric glial cells following intestinal ischemia and reperfusion. Acta Histochem. https://doi.org/10.1016/j.acthis.2022.151985
Nooh HZ, Nour-Eldien NM (2016) The dual anti-inflammatory and antioxidant activities of natural honey promote cell proliferation and neural regeneration in a rat model of colitis. Acta Histochem 118:588–595. https://doi.org/10.1016/j.acthis.2016.06.006
Ochoa-Cortes F, Turco F, Linan-Rico A et al (2016) Enteric glial cells: a new frontier in neurogastroenterology and clinical target for inflammatory bowel diseases. Inflamm Bowel Dis 22:433–449. https://doi.org/10.1097/MIB.0000000000000667
Palombit K, Mendes CE, Tavares-de-Lima W et al (2019) Blockage of the P2X7 receptor attenuates harmful changes produced by ischemia and reperfusion in the myenteric plexus. Dig Dis Sci. https://doi.org/10.1007/s10620-019-05496-8
Peng W, Cotrina ML, Han X et al (2009) Systemic administration of an antagonist of the ATP-sensitive receptor P2X7 improves recovery

after spinal cord injury. Proc Natl Acad Sci USA 106:12489–12493. https://doi.org/10.1073/pnas.0902531106

Poli E, Lazzaretti M, Grandi D et al (2001) Morphological and functional alterations of the myenteric plexus in rats with TNBS-induced colitis. Neurochem Res 26:1085–1093. https://doi.org/10.1023/A:1012313424144

Rühl A (2005) Glial cells in the gut. Neurogastroenterol Motil 17:777–790. https://doi.org/10.1111/j.1365-2982.2005.00687.x

Sanovic S, Lamb DP, Blennerhassett MG (1999) Damage to the enteric nervous system in experimental colitis. Am J Pathol 155:1051–1057. https://doi.org/10.1016/S0002-9440(10)65207-8

Santos AAQA, Costa VS, Martins S et al (2022) P2X7 receptor blockade decreases inflammation, apoptosis, and enteric neuron loss during *Clostridioides difficile* toxin A-induced ileitis in mice. World J Gastroenterol 28:4075–4088. https://doi.org/10.3748/wjg.v28.i29.0000

Schneider J, Jehle EC, Starlinger MJ et al (2001) Neurotransmitter coding of enteric neurones in the submucous plexus is changed in non-inflamed rectum of patients with Crohn's disease. Neurogastroenterol Motil 13:255–264. https://doi.org/10.1046/j.1365-2982.2001.00265.x

Souza RF, Evangelinellis MM, Mendes CE et al (2020) P2X7 receptor antagonist recovers ileum myenteric neurons after experimental ulcerative colitis. World J Gastrointest Pathophysiol 11:84–103. https://doi.org/10.4291/wjgp.v11.i4.84

Valès S, Touvron M, Van Landeghem L (2018) Enteric glia: diversity or plasticity? Brain Res 1693:140–145. https://doi.org/10.1016/j.brainres.2018.02.001

Venkataramana S, Lourenssen S, Miller KG, Blennerhassett MG (2015) Early inflammatory damage to intestinal neurons occurs via inducible nitric oxide synthase. Neurobiol Dis 75:40–52. https://doi.org/10.1016/j.nbd.2014.12.014

Von Boyen G (2011) The role of enteric glia in gut inflammation. Neuron Glia Biol 21:1–6

Wirtz S, Neufert C, Weigmann B, Neurath MF (2007) Chemically induced mouse models of intestinal inflammation. Nat Protoc 2:541–546. https://doi.org/10.1038/nprot.2007.41

Yiangou Y, Facer P, Baecker PA et al (2001) ATP-gated ion channel P2X3 is increased in human inflammatory bowel disease. Neurogastroenterol Motil 13:365–369. https://doi.org/10.1046/j.1365-2982.2001.00276.x

Zhou J, Lai W, Yang W et al (2018) BLT1 in dendritic cells promotes Th1/Th17 differentiation and its deficiency ameliorates TNBS-induced colitis. Cell Mol Immunol 15:1047–1056. https://doi.org/10.1038/s41423-018-0030-2

Ziegler U, Groscurth P (2004) Morphological features of cell death. News Physiol Sci 19:124–128. https://doi.org/10.1152/nips.01519.2004